

# EXPERIMENTAL EVALUATION OF SEISMIC RESISTANT BEAM-COLUMN T-JOINTS OF RIGID-FRAME BRIDGE UNDER CYCLIC LOADING

Kabir SHAKYA<sup>\*1</sup>, Ken WATANABE<sup>\*2</sup> and Junichiro NIWA<sup>\*3</sup>

## ABSTRACT

This paper represents the experimental results of one-sixth scale beam-column joint which is constructed according to the existing design of rigid-frame bridges in Japan. Displacement controlled quasi-static horizontal reversal load was applied to investigate the failure mechanism and the shear capacity. The test results showed that the flexure failure of beam nearby joint occurred prior to the failure of beam-column joint. The internal damage which was not visible from outside occurred inside the beam-column joint due to excessive strain in beam rebars.

**Keywords:** beam-column joint, drift ratio, quasi-static reversal load, rigid-frame bridge, strain

## 1. INTRODUCTION

The extensive researches conducted on bridges during past two decades resulted significant modification in seismic provisions of codes in different countries around the world. The previous studies mainly revealed some of the major deficiencies in old bridges, such as inadequacies in: flexural strength due to small base shear, flexural ductility due to insufficient transverse reinforcement, and flexural capacity at the column-footing zone due to short length lap-splice, detailing at beam-column joints because of lack of hooks in beam steel reinforcement and also due to absence of hoops at joints. Shear failure in columns, confinement failure in the flexural plastic hinge region, sliding failure of lap-spliced reinforcement at the lower end of columns and joint shear failure were common in the bridges.

Caltrans seismic design practice requires essentially the elastic behavior in the superstructure and recommends columns, pier walls, backwalls, seismic isolation, damping devices and shear keys to show inelastic behavior [1]. The locations within the bridge for the formation of plastic hinges are pre-determined so that the inspection and the repair can be done easily. Formation of plastic hinges in column or pier enables significant energy dissipation under the severe deformations during large seismic events. Hence, desired locations of plastic hinge should be identified, designed and detailed for ductile response. In Japan, a large number of rigid-frame bridges have been constructed (Fig. 1). In these bridges, intermediate link beams tie the columns together enhancing the stability and stiffness of the structures but are not subjected to vertical loads from superstructures. Although in real structures, beams are connected to columns in two or

more faces (i.e. 3-D) but for simplicity 2-D system can be chosen.

The main objective of the research is to optimize the amount of steel reinforcement in existing design of railway bridges. The presented paper focuses on finding out the failure mechanism and examining the load capacity of the one-sixth scale beam-column T-joint of existing railway bridge. Strain in longitudinal rebars and the slip amount of beam longitudinal rebars were used as a measure to determine the deterioration of the beam-column joint. The failure mechanism was evaluated by observing the crack pattern. Load-displacement, base shear-drift ratio and moment-rotation relationships were also used to understand the structural behavior.

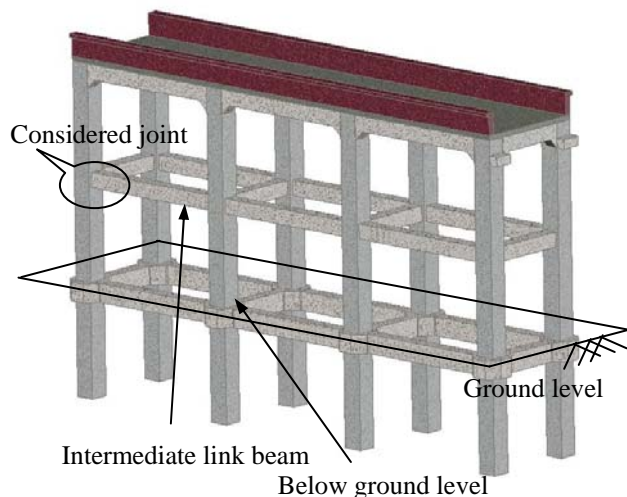


Fig. 1 Rigid-frame bridge.

\*1 Ph.D. student, Dept. of Civil Engineering, Tokyo Institute of Technology, JCI Member

\*2 Assistant Prof., Dept. of Civil Engineering, Tokyo Institute of Technology, Ph.D., JCI Member

\*3 Prof., Dept. of Civil Engineering, Tokyo Institute of Technology, Dr. Eng. JCI Member

## 2. PREVIOUS RESEARCHES

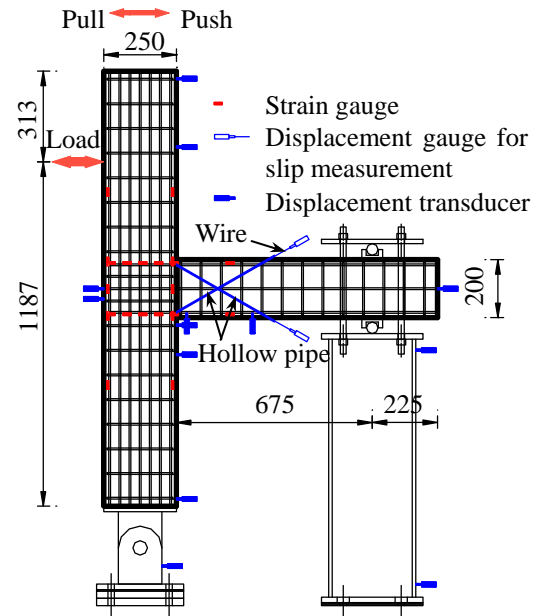
A method to predict the ductile capacity of reinforced concrete beam-column joints failing in shear after the development of plastic hinges at both ends of the adjacent beams was developed [2]. The effect of longitudinal axial strain of a beam in the plastic hinge region of the beam on the joint longitudinal strain was also included. The enhancement of the joint capacity in terms of ductility and the shear capacity were observed when two types of retrofit namely, addition of reinforced concrete bolsters and addition of post-tensioned reinforced bolsters to the beam, were done [3]. The load path and the inelastic material behavior highly affect the design strengths during unidirectional and bidirectional loading [4]. The effects in design strengths can be verified by the analytical and experimental results of beam-column connection. With variation in steel reinforcement arrangement at beam-column joints causes different mechanisms of shear transfer in knee and T-joints [5].

## 3. TEST SETUP AND INSTRUMENTATION

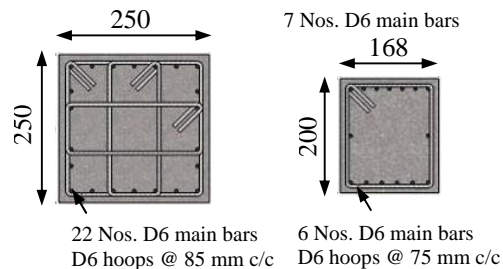
### 3.1 Test specimen and materials

The experiment was carried out on one-sixth scale specimen which was prepared based on the existing rigid-frame railway bridges in Japan (prototype structure for this research). Figure 2 shows the specimen details comprising of a junction between a column and an intermediate link beam. The height of column is considered as 1500 mm and the length of beam from the face of column to the end was considered as 900 mm. The cross-sectional sizes of column and beam were 250 mm × 250 mm and 168 mm × 200 mm, respectively. The arrangement of longitudinal and transverse reinforcements in column and beam are shown in Fig. 2, where 22 numbers of main bars with hoops spaced at 85 mm center to center were provided in the column and 15 numbers of main bars with stirrups spaced at 75 mm center to center were provided in the beam.

The material properties between the specimen and a prototype structure are compared in Table 1. In a prototype, longitudinal bars of diameter 32 mm were used, however, steel bars of 6 mm diameter were adopted in the test specimen in order to maintain same number of reinforcing bars in a prototype structure and the test specimen. The rebars from beam, column and



(a) Bar arrangement and measurement system.



(b) Cross section of column. (c) Cross section of beam.

Fig. 2 Specimen details.

Table 1 Comparison of material properties between test specimen and prototype structure.

(a) Reinforcement

Specimen	Bar size	Stirrup size	$f_y$ (N/mm <sup>2</sup> )	Percentage of steel (%)			
				Column		Beam	
				Longitudinal reinforcement	Tie Bar	Longitudinal reinforcement	Stirrup
Test specimen	D6	D6	295	0.99	0.571	1.181	0.443
Prototype structure	D32	D16	390	0.96	0.574	1.27	0.643

(b) Concrete

Specimen	$f'_c$ (N/mm <sup>2</sup> )	Max. aggregate (mm)	Slump (cm)	W/C	Air content	Mix proportion (kg/m <sup>3</sup> )			
						Coarse		Fine	
						Cement	Aggregate	aggregate	Water
Test specimen	39.8	10	8	0.6	4.0%	291	436	811	174
Prototype structure	30	25	8	0.55	4.5%	291	-*	-*	160

\* Data not available

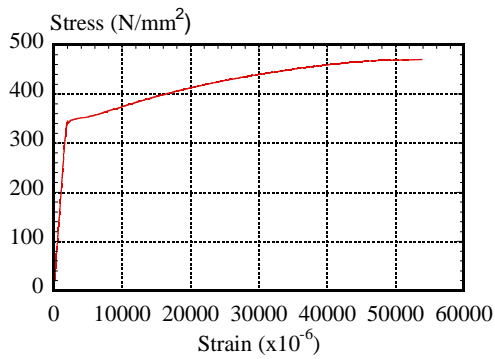


Fig. 3 Stress-strain curve of D6 rebar.

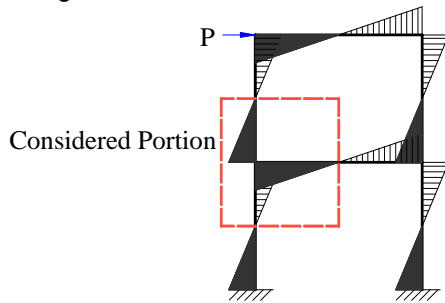


Fig. 5 Moment in frame due to lateral load.

tie bars caused congestion at the joint due to which there was difficulty in casting. The clear spacing between column bars was 29 mm and that in beam was 16 mm. The clear spacing was enough for the passage of aggregates. Three numbers of 100 mm × 200 mm and two numbers of 150 mm × 250 mm cylinders were cast and cured for compressive strength and tensile splitting tests, respectively. The average modulus of elasticity, average compressive strength and average tensile splitting strength were found to be 26.3 kN/mm<sup>2</sup>, 39.8 N/mm<sup>2</sup>, and 2.4 N/mm<sup>2</sup>, respectively. The tensile test of D6 bar was also performed. The stress-strain curve of D6 bar is shown in Fig. 3. The yield strength and the ultimate strength were found to be 325 N/mm<sup>2</sup> and 470 N/mm<sup>2</sup>, respectively. The yield strain was 1750 × 10<sup>-6</sup>. Based on this stress-strain curve, the yielding of rebars during the loading test was judged.

### 3.2 Test setup and measurement system

A structural framework was arranged to support the specimen. An axial load in the column was neglected assuming that lateral load effects were significant compared to vertical load. Also, the axial load due to bridge superstructure is not very high unlike in buildings. Using a 200 kN capacity displacement controlled hydraulic actuator, a cyclic horizontal quasi-static load (Fig. 4) was applied on the column. The amplitudes of displacement were varied from 0.5 mm to 70 mm and loading rates were also varied. Three cycles of each displacement amplitude were exerted.

The T shaped specimen with pin support at column and roller support at the beam (Fig 2(a)) was selected. The shape, size and the boundary condition of the specimen was chosen by examining the structural behavior of portal frame subjected to lateral load. On applying lateral load, the moment diagrams at the considered portion of portal frame (Fig 5) and the

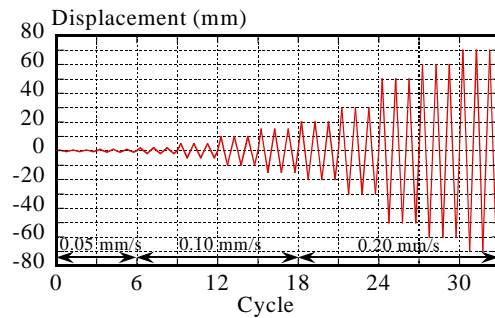


Fig. 4 Applied displacement cycle and loading speed.

specimen were similar. In a specimen, the bottom of the column was pinned to the loading frame and the beam end attached with a roller was rested on a steel column which was strongly connected to the loading frame. To ensure the fixity of supports, prestressing forces were applied on the support plates. These supports allowed a rotation of both column and beam and fixed the vertical movement. However, free horizontal movement of the beam was permitted.

In order to record and understand structural behavior such as strains, deformations and cracking patterns under cyclic loading, adequate measurement system, as shown in Fig. 2(a), was installed in the experimental setup. The strain gauges were installed on both horizontal and vertical reinforcements at the beam-column joint. Also, in column and beam longitudinal rebars, strain gauges were attached at a distance of effective depth of column and beam, respectively from the corresponding faces. In order to measure the bar slip, displacement gauges were attached to the longitudinal bars of a beam located at the face of the column. The vertical and horizontal displacements at various locations of a specimen were measured using displacement transducers. To measure large displacements, wire type displacement transducers were attached at different places. Transducers were attached in the steel column and hinge support as well, so that the displacement of supports can be monitored. If supports are displaced, correction in displacement at other locations can be considered. Gauges were also pasted at the concrete surface to measure the strain at various locations.

## 4. EXPERIMENTAL RESULTS AND DISCUSSION

### 4.1 Crack pattern

First crack was observed during the first cycle of 10 mm amplitude displacement. Opening and closing of cracks including formations of new cracks were continued till 50 mm displacement amplitude was applied. However, on further loading only opening and closing of cracks were observed which eventually caused spalling of concrete during 60 mm displacement amplitude. Most of the cracks were highly concentrated at the beam near the column face. Very few cracks were observed in the column. The crack pattern in the specimen till the 3rd cycle of 70 mm displacement is shown in Fig. 6. In the figure, the first two digits



were deteriorated. The cracks around the rebars were comparatively small and were not extended to the surface.

#### 4.4 Load-displacement and base shear-drift ratio relationships

Load-displacement curve of column at the level of actuator, obtained from the quasi-static reversal loading is shown in Fig. 12. Relatively smooth hysteresis loops were observed for the displacement amplitude up to 30 mm. However, for 50 mm and above displacement amplitudes, some spikes were formed in the hysteresis loops. The presence of frictional forces at the roller support caused some obstruction in smooth rolling of rollers. At higher displacement amplitudes, rollers started to skid instead of rolling due to the movement of roller supporting plates as shown in Fig. 13 and it resulted in formation of spikes in the hysteresis loops. Besides, low magnitude of load capacity is observed when the specimen was pulled towards the actuator than that during pushing the specimen away from the actuator. The effect of roller supporting plates was investigated by FEM analysis and found that the load capacity was increased due to restriction of roller movement. However, it did not highly affect the overall objective of the research.

The peak loads in each displacement amplitude are marked in Fig. 12. The load capacity of the

specimen increased linearly till the first crack was formed at first cycle of 10 mm displacement. The cracks were rapidly developed after the appearance of the first crack and some beam rebars were yielded during the first cycle of 15mm displacement. As a result, no significant increase in load capacity was observed on increasing horizontal displacement. However, drastic increase in load capacity was observed when the specimen was displaced by 50 mm. The drastic increase in load capacity was due to friction on roller and the difference in fixity level of supporting steel plates of rollers above and below the beam. No new cracks were developed after 50 mm horizontal displacement. Spalling of concrete and buckling of beam longitudinal rebars were observed during 60 mm horizontal displacement. On further pulling the specimen towards the actuator, the load capacity became almost constant. But same tendency was not observed when the specimen was pushed away from the actuator. At the first cycle of 70 mm displacement amplitude, the load capacities were found to be 42.2 kN and 53.2 kN during pulling and pushing, respectively. The load capacity decreased on further loading cycles. The shear force at the beam-column joint was calculated following the method recommended by ACI 352R-02 [6] and it was found to be 48.5 kN. The joint shear capacity was also calculated and was found to be 284.8 kN. Hence, the design of joint is too conservative and steel reinforcement at the joint can be reduced. However,

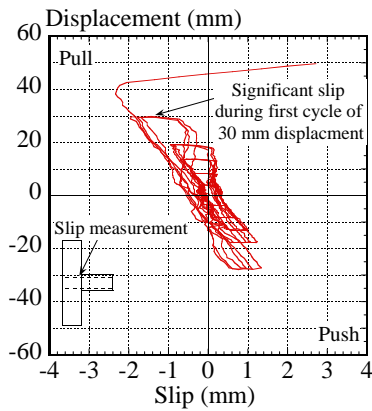


Fig. 10 Displacement-slip relationship.

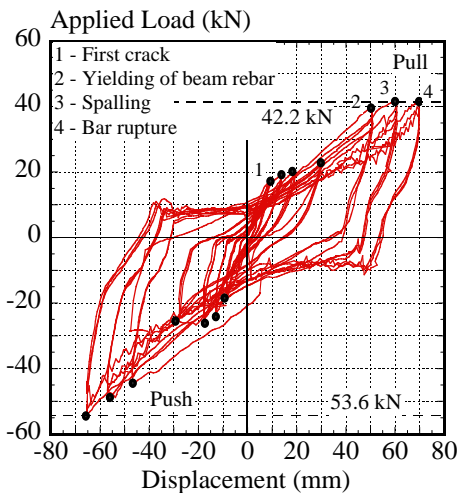


Fig. 12 Load-displacement curve.

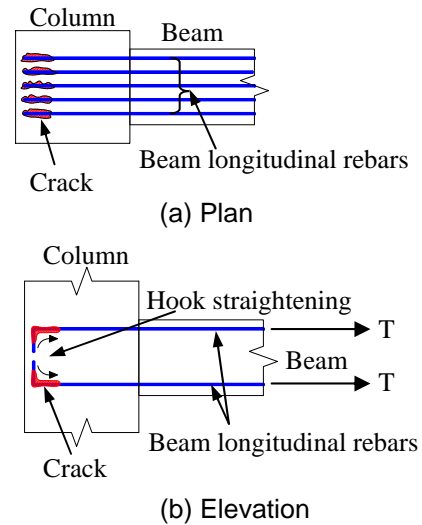


Fig. 11 Slipping of rebars.

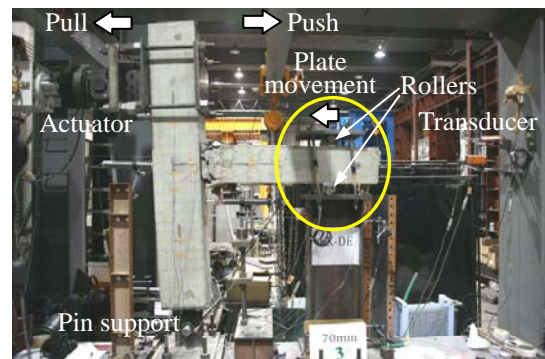


Fig. 13 Displacement of roller supporting plate.

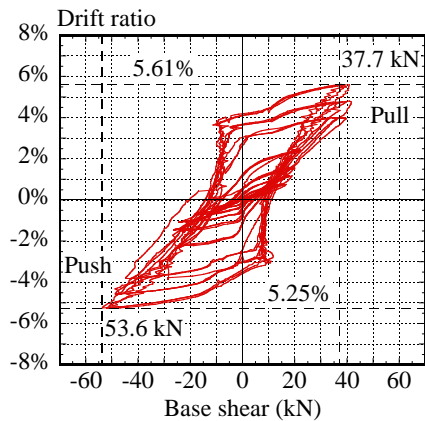


Fig. 14 Base shear versus drift ratio relationship.

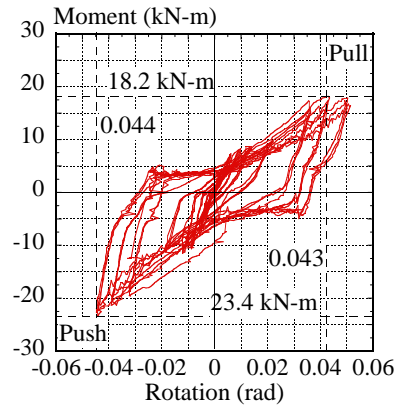


Fig. 15 Moment-rotation curve.

overall structural behavior should be checked. Although the flexural failure of beam can be shown through calculations, the experiment was conducted in order to compare the behavior of existing structure with modified structure with reduced steel rebars and reinforced with steel fibers.

The response of the specimen is also expressed in terms of base shear and drift ratio. Drift ratio is defined as the ratio of displacement at the top of column relative to the bottom of the column to the height between those points. The relationship between base shear and drift ratio is shown in Fig. 14. The base shears of 37.7 kN and 53.6 kN were noticed as limiting base shears when the maximum drift ratio of 5.61% and 5.25% during pulling and pushing were applied. At these drift ratios, concrete spalled and buckling of longitudinal beam rebars including rupture of two beam rebars due to which it was decided to stop the experiment. Hence, the damage at these drift ratios was considered as the irreparable damage.

#### 4.5 Moment-rotation curve

From the measured displacements at the top and the middle height of column, the rotation of column was calculated. The moment-rotation curve for column is plotted in Fig. 15. When the specimen was pulled towards actuator, maximum moment of 18.2 kN-m corresponding to the rotation of 0.043 rad was found during application of first cycle of 60 mm displacement amplitude. Similarly, during application of first cycle of 70 mm displacement amplitude, maximum moment of 23.4 kN-m and corresponding rotation of 0.044 rad were observed upon pushing the specimen. The magnitude of moment in pulling direction is smaller than that in pushing of specimen because of movement of supporting plates of rollers (Fig. 13) and the formation of plastic hinge in the beam.

#### 5. CONCLUSIONS

A one-sixth scale beam-column joint is constructed following the existing rigid-frame bridge in Japan and tested under displacement controlled quasi-static horizontal cyclic load. Based on the experimental results following conclusions are obtained:

- (1) In the considered specimen, beam-column joint was stronger than the beam as plastic hinge was formed in beam before failure of joint.
- (2) Bond deterioration within beam-column joint caused tensile force in compression steel in the beam during reversal loading.
- (3) The excessive strain in beam rebars indicated the internal damage of beam-column joint though no significant cracks on surface were visible.
- (4) The shear capacity of beam-column joint was too high than the applied shear at the joint and it indicates the conservative design of the joints.
- (5) On the basis of test results, it can be said that in real structures of considered type, the flexural failure will occur in the beams prior to beam-column joints failure during seismic events.

#### REFERENCES

- [1] Caltrans Technical Publications, Memo to Designers, <http://www.dot.ca.gov/hq/esc/techpubs/manual/bri dgemanuals/bridge-memo-to-designer/bmd.html>, (Date: 2009-12-12).
- [2] J. Y. Lee, J. Y. Kim and G. J. Oh: Strength Deterioration of Reinforced Concrete Beam-Column Joints Subjected to Cyclic Loading, *Engineering Structures*, Vol. 31, pp. 2070-2085, Apr. 2009.
- [3] L. N. Lowes and J. P. Moehle: Evaluation and Retrofit of Beam-Column T-Joints in Older Reinforced Concrete Bridge Structures, *ACI Structural Journal*, Vol. 96, pp. 519-533, Jul.-Aug. 1999.
- [4] S. Mazzoni and J. P. Moehle: Seismic Response of Beam-Column Joints in Double-Deck Reinforced Concrete Bridge Frames, *ACI Structural Journal*, Vol. 98, pp. 259-269, May-Jun. 2001.
- [5] M. J. N. Priestley, F. Seible and G. M. Calvi: *Seismic Design and Retrofit of Bridges*, John Wiley and Sons, Inc., 1996.
- [6] Joint ACI-ASCE Committee 352: *ACI 352R-02, Recommendations for Design of Beam-Column Connections in Monolithic Reinforced Concrete Structures*, 2002.